Chapter-V

Sorption studies of cationic dye methylene blue over CHA/NiAl-LDH adsorbent

Chapter-V

Sorption studies of cationic dye methylene blue over CHA/NiAl-LDH adsorbent

V.1 Introduction

Textile industry is one of the major industries that discharges effluents containing various toxic dyes, chemicals, and heavy metals into natural water bodies such as lakes, oceans, canals, and rivers.[1,2] Among these contaminants, dyes are widely used globally and considered as toxic when come in contact with living organism, depending on exposure time and concentration. In particular, methylene blue (MB) is one of the most commonly used dyes in the textile industry for colouring and various medical and biological applications. It is a cationic dye with a complicated structure, and removing it from the effluent is a very difficult task.[3,4] Despite the fact that MB dye has been demonstrated to possess certain medicinal properties, the discharge of partially or untreated MB dye-loaded waste water from industrial sources poses a number of health hazards. For instances, MB dye can cause cyanosis, tissue necrosis, jaundice, vomiting, and Heinz body development, etc. Thus, it is highly imperative to eliminate MB dye from waste water.[5-7]

With an emphasis on the development of a new hybrid material for the removal of the organic dye methylene blue from an aqueous solution. In this work, we have synthesized the composite material of NiAl-LDH and coconut husk ash and tested its adsorption efficiency. This hybrid material combines the advantages of both adsorbents. Various isotherm models and kinetic models were applied to investigate the removal mechanism of MB.

V.2 Experimental section

V.2.1 Materials and Methods

Nickel chloride hexahydrate ($NiCl_2.6H_2O$), Aluminium chloride ($AlCl_3$), Sodium Hydroxide (NaOH), and Methylene blue ($C_{16}H_{18}ClN_3S$) were purchased from Merck. The quality of all the obtained chemicals is of analytical grade and was applied directly during the experiment without further purification. All the standard solutions in the experiment are prepared by using deionised water.

V.2.2 Synthesis of the adsorbent CHA/NiAl-LDH

The CHA-modified NiAl-LDH was synthesized via the co-precipitation method, as mentioned in the previous chapter IV. The coconut husk was heated in a muffle furnance at 500 ℃ for 4 hours. And the obtained ash, labelled as CHA, was collected. A solution of 100 mL containing a mixture of 0.1 M $AlCl_3$ and 0.2 M $NiCl_2.6H_2O$ is continuously stirred in a magnetic stirrer for 10 minutes until a clear solution was obtained. 3 g of the CHA is mixed in the resulting solution and was co-precipitated by adding 2 M NaOH solution at room temperature. The precipitate obtained is allowed to agitate in a magnetic stirrer for 6 hours and further separated by centrifugation. The obtained black precipitate was washed several times with distilled water, and the resulting slurry was dried at 50 ℃ in an oven and powdered. The final modified product was labelled as CHA/NiAl-LDH.

V.2.3 Adsorption Experiment

The experimental adsorption isotherm procedure for the sorption of methylene blue on the synthesized adsorbents was carried out via the batch method. An adsorbent of fixed mass (0.035 g) was added to the 20 mL solution of methylene blue dye of known concentration ranging between 10 and 55 mg/L. The dye solution is allowed to agitate in a thermostatic shaker for a time period of 4 hours to attain equilibrium stage. The liquid sample is filtered to separate the adsorbent, and the filtrate obtained is used for measuring the residual dye concentration in UV-visible spectrophotometer at 655 nm wavelength.

The equilibrium adsorption capacity (q_e) and the % of dye removal were evaluated with following formula:

$$\% \text{ of dye removal} = \frac{(C_0 - C_e) \times 100}{C_0} \tag{5.1}$$

$$q_e = \frac{(C_0 - C_e)\, V}{W} \tag{5.2}$$

where, C_0 and C_e denotes initial and equilibrium dye concentration, respectively. q_e indicates the amount of dye adsorbed at equilibrium, V represents volume of the adsorbate solution (mL) and W signifies the quantity of adsorbent (g).

In the kinetic experiment approximately 40 mL of dye solution with an initial concentration of 10 mg/L was taken in a conical flask, and 0.3 g of the adsorbent was dispersed in the solution. Similarly, the resulting solution is then shaken in a thermostatic shaker, and 2 mL of the liquid solution is withdrawn after a definite time interval. The kinetics experiment was studied from 0 to 200 minutes. Again, the adsorbent is separated by filtration, and the absorbance value of the filtrate was measured.

The quantity of dye adsorbed at time *t* is presented by the equation:

$$q_t = \frac{(C_0 - C_t)\,V}{W} \qquad (5.3)$$

V.3. Results and Discussion

V.3.1 Characterization of the adsorbents

V.3.1.1 Powder X-ray Diffraction

X-ray diffraction (XRD) is a primary characterization technique based on the principle of Braggs equation, which can be described in terms of reflection of collimated x-ray beam incidence on a crystal plane of the sample that needs to be characterized. Moreover, analysis of a sample by PXRD provides important information that is complementary to various microscopic and spectroscopic methods, such as phase identification, sample purity, crystallite size and morphology. The X-ray diffraction patterns of CHA and CHA/NiAl-LDH are presented in **Fig V.1**. The pristine NiAl-LDH showed six peaks corresponding to the indexed plane (003), (006), (009), (015), (018), and (110), which infers the formation of typical LDH structures.[7] In modified CHA/NiAl-LDH, similar peaks of pristine LDH are observed in addition to the peaks of CHA, which appear at the diffraction angle 2θ value of 20.7, 21.99, 26.5, 28.1, 29.5, 35.6, 39.3, 42.3, 45.5, 49.9, and 68.1. Thus, it suggests that the coconut husk ash (CHA) has been well and successfully assembled in the LDH structure. However, the calculated values of LDH cell parameters a = 3 Å and c = 23.1 Å in both NiAl-LDH and CHA/NiAl-LDH are the same, which revealed that the structure of LDH is not distorted. Therefore, the obtained results are consistent with the previously reported result.[8]

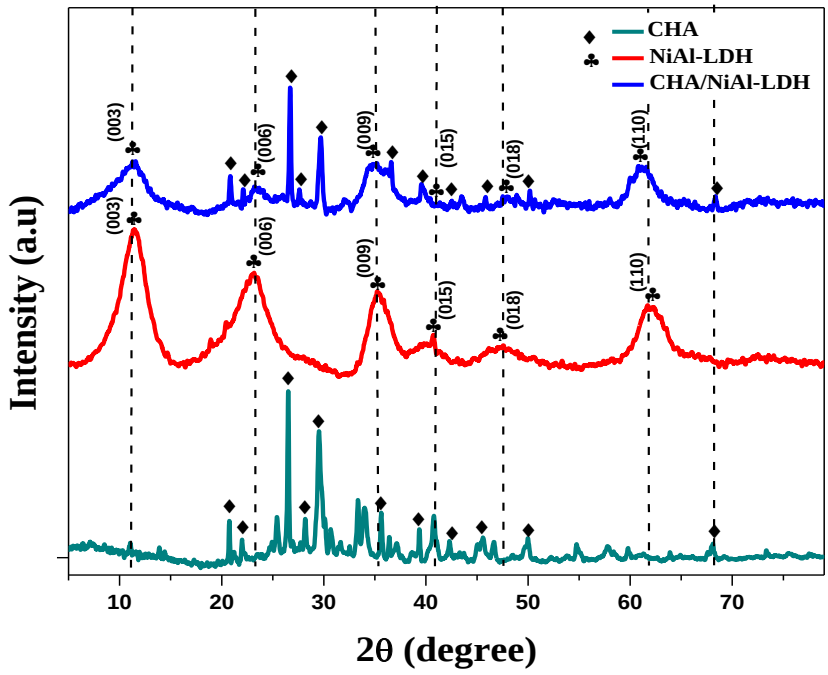

Fig V.1: PXRD pattern of CHA, NiAl-LDH and CHA/NiAl-LDH.

V.3.1.2 FT-IR analysis

Fourier transform spectroscopy (FTIR) is an established technique for studying the surface of various materials including organic and inorganic materials. This technique provides information about functional groups of the layered materials, giving a molecular fingerprint of the materials. Consequently, inorder to get detailed insight on structural functional groups, FTIR spectroscopy has been used to investigate the structure of CHA and CHA/NiAl-LDH composite. The FT-IR spectra of CHA and CHA/NiAl-LDH were depicted in **Fig V.2**. CHA showed peaks at 3443 (-OH), 1631 (C=C), 1591 (C-O group of skeletal aromatics), 2920 (C-H), and 1143 cm^{-1} (C-O stretch of ester, phenol, and ether). After compositing with LDH, the adsorbent CHA/NiAl-LDH showed new additional peaks at 1028 cm^{-1} and 1403 cm^{-1}. The M-O stretching vibrations such as Ni-O, Al-O, Si-O, Ca-O, K-O, etc., were observed in the lower frequency region between (400-1000) cm^{-1}. [9,10]

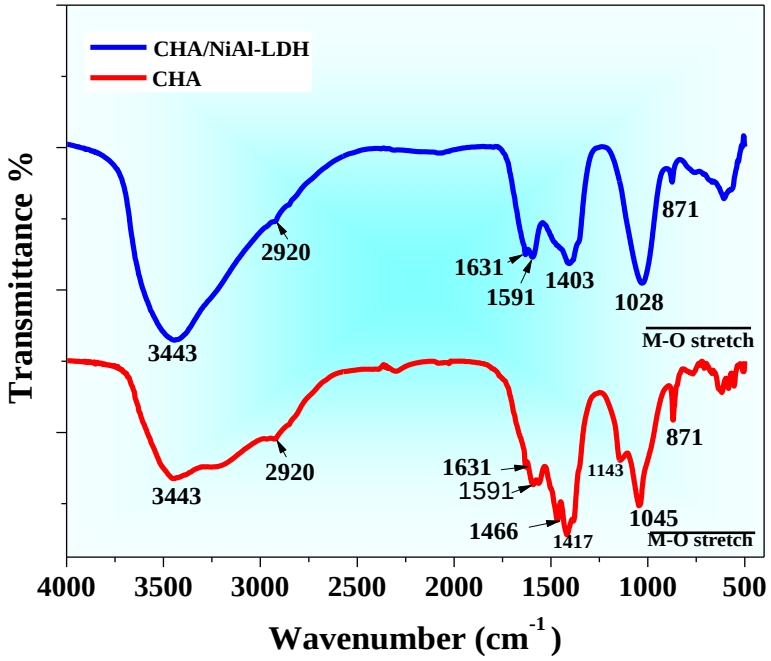

Fig V.2: FT-IR spectra of CHA and CHA/NiAl-LDH.

V.3.1.3 Surface area, pore size and pore volume analysis

Critical to the designing and synthesis of solid materials, surface area analysis by BET (Brunauer-Emmett-Teller) technique is one of the most widely used methods in material characterization. It is the multipoint measurement of analytes specific surface area through gas adsorption analysis. The surface properties of CHA and CHA/NiAl-LDH such as pore size, pore volume, and surface area, were investigated using the N_2 adsorption-desorption isotherm obtained from the Quantachrome Novawin analyser at 77 K. The insets of **Fig V.3(a)** and **Fig V.3(c)** show the adsorption-desorption isotherm curves of CHA and CHA/NiAl-LDH, which are characteristics of type-IV isotherms, and the generated hysteresis loop revealed type III based on the IUPAC classification.[11] Moreover, the average pore sizes of CHA and CHA/NiAl-LDH as presented in **Fig V.3 (b)** and **Fig V.3 (d)** were 4.48 and 3.23 nm, respectively. Thus, it indicates the presence of mesopores on the adsorbent surfaces. In addition, the specific surface areas exhibited by CHA and CHA/NiAl-LDH were 20.71 and 4.17 m^2/g, respectively.

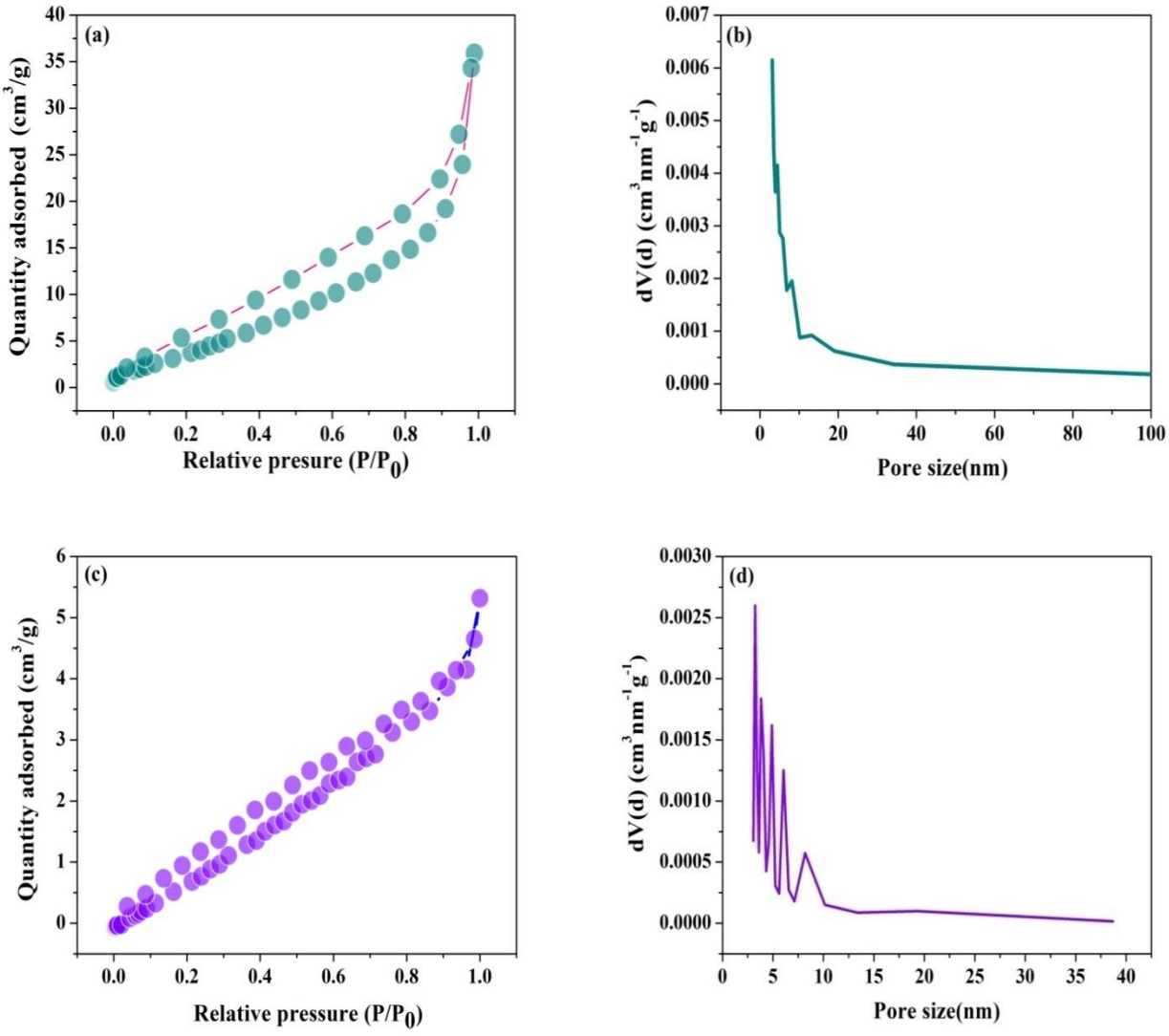

Fig V.3: N_2 adsorption-desorption isotherm of CHA (a) and CHA/NiAl-LDH (c). Pore size distribution plot of CHA (b) and CHA/NiAl-LDH (d)

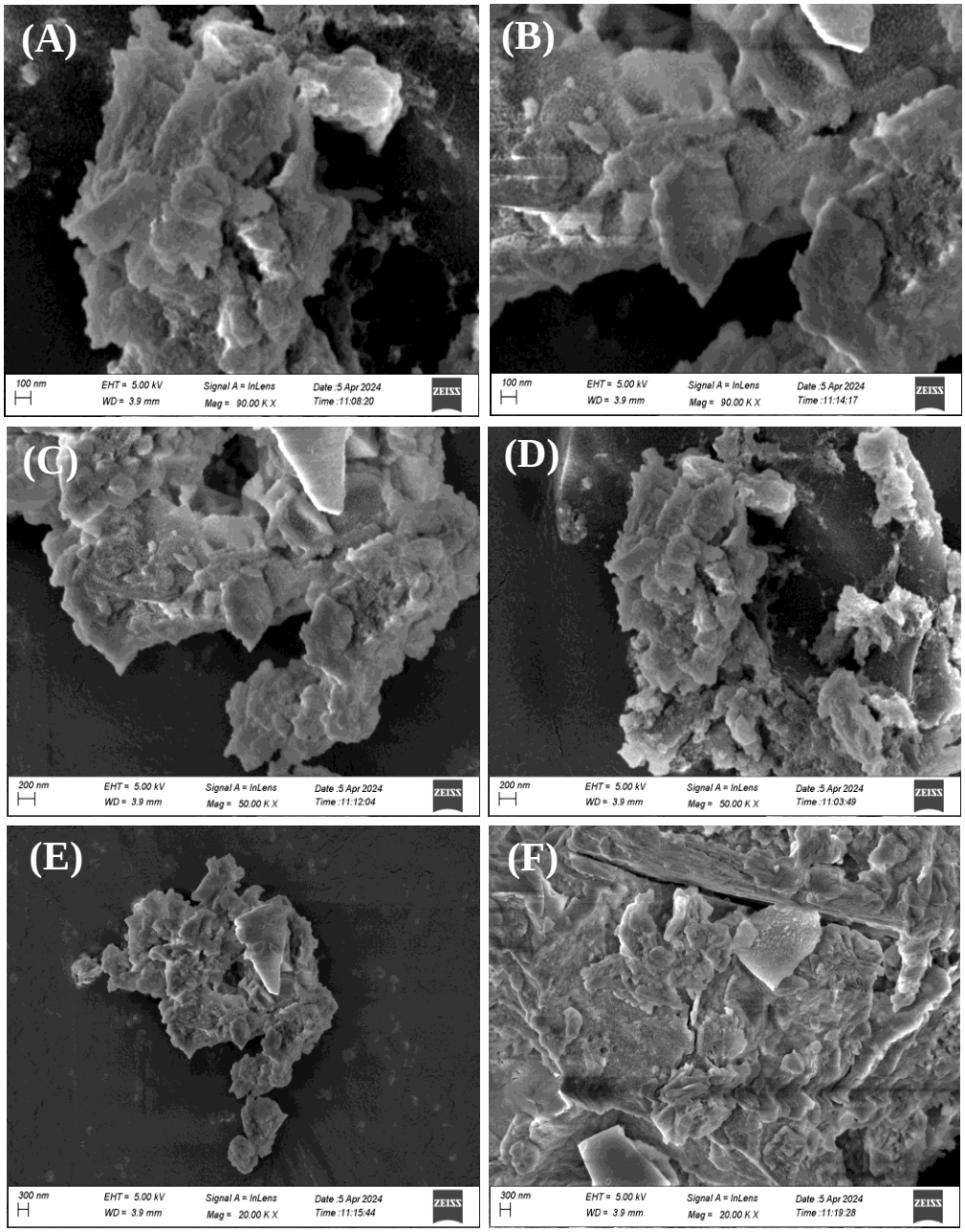

Fig V.4: FE-SEM images of CHA/NiAl-LDH composite.

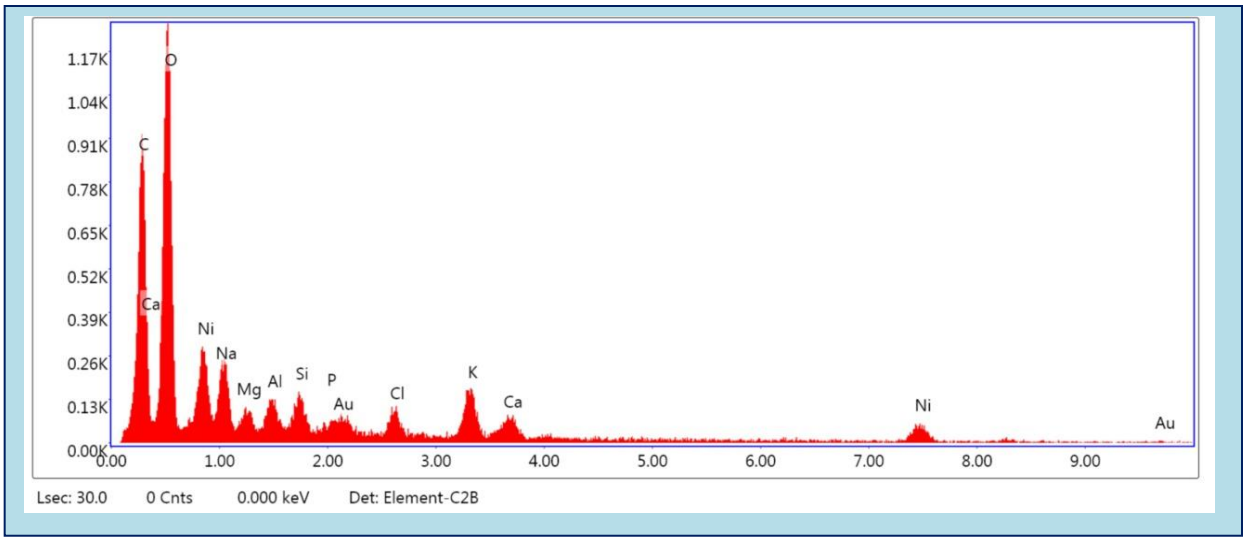

Fig V.5: EDX spectra of CHA/NiAl-LDH composite.

V.3.1.4. SEM-EDX Analysis

Field emission scanning emission microscopy (FESEM) is a powerful analytical technique to perform analysis on a wide range of materials, at high magnifications and to produce high resolution images. It is very helpful in investigating the external surface morphology of materials in micro and nano range. As a result, the surface morphology of the as-synthesized composite was visualized at 100 nm, 200 nm and 300 nm scale size. **Fig V.4(A-F)** displays the FE-SEM images of the CHA/NiAl-LDH composite. The formation of sheet-shaped LDH particles was observed in **Fig V.4 (A,B,C**), whereas the structure of carbonaceous ash material in CHA/NiAl-LDH revealed the appearances of pores with a smooth cylindrical surface. Moreover, the LDH platelets remained deposited over the surface of coconut husk ash in the composite material. Besides, to ensure the successful formation of the composite material the distribution of the elements and composition was analyzed with EDS (**Fig V.5**). EDX results determined the presence of constituent elements C, O, Na, Mg, Al, Si, P, Ni, K, Ca, and Cl with 24, 40, 6.64, 1.36, 1.99, 1.94, 0.51, 9.63, 5.74, 2.71, and 2.12 %, respectively. Elemental mapping depicted in **Fig V.6** also showed the well distributed constituent elements in the adsorbent CHA/NiAl-LDH.[12]

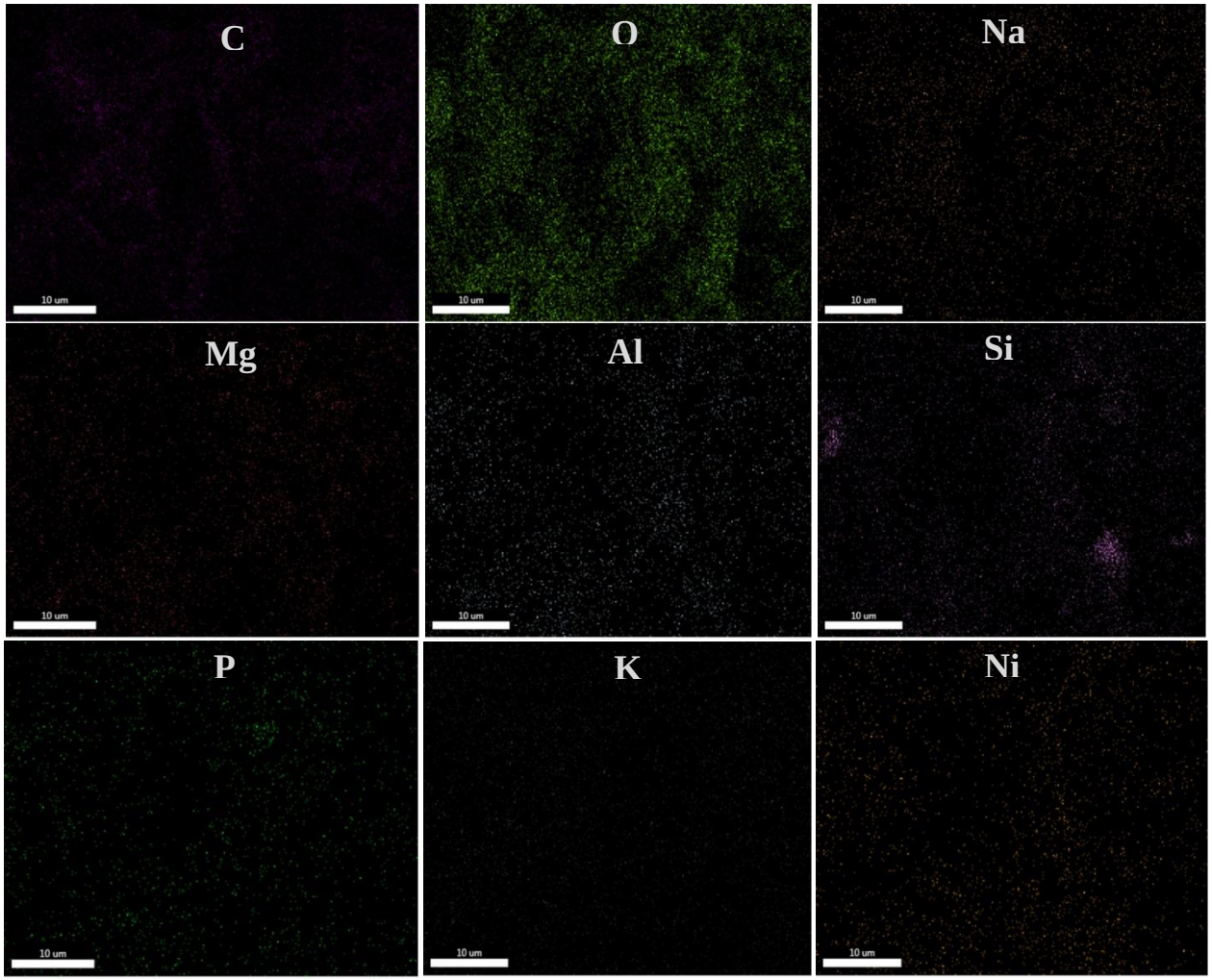

Fig V.6: Elemental mapping of few elements detected on CHA/NiAl-LDH.

V.3.2 Effect of Temperature

The thermodynamic experiment for the adsorption of MB onto CHA and CHA/NiAl-LDH was performed at 40 ℃, 50 ℃, and 60 ℃. In addition, the various thermodynamic parameters, such as ΔH, ΔG, and ΔS were calculated to predict the nature of the adsorption process, such as spontaneity and the surface of the adsorbent. These parameters can be accessed through the following equations:[13,14]

$$\ln K_d = \frac{\Delta S}{R} - \frac{\Delta H}{RT} \quad (5.4)$$

$$\Delta G = -RT \ln K_d \quad (5.5)$$

where, ΔH and ΔS signifies standard enthalpy and standard entropy, respectively, ΔG represents standard free energy, K_d is the adsorption distribution coefficient, R and T are universal gas constant and temperature (K), respectively.

The graphical representation of the Vant-Hoff plot (ln K_d vs 1/T) is displayed in **Fig V.7**. The standard entropy ΔS and enthalpy ΔH values are measured from the respective intercept and slope of the plot. The detailed thermodynamic parameters obtained are listed in **Table V.1**. The estimated values of ΔH for CHA and CHA/NiAl-LDH are 29.26 and 24.60 KJ/mol, respectively. However, the positive value of ΔH confirms the endothermic process of adsorption, and the negative Gibbs free energy ΔG indicates spontaneity of the sorption process.[15]

TableV.1: Thermodynamic parameters for adsorption of methylene blue on CHA and CHA/NiAl-LDH.

Adsorbent	**+ΔH(KJ/mol)**	**+ΔS(J/mol)**	**ΔG(KJ/mol)**		
			313 K	323 K	333 K
CHA	29.26	100.27	-2.103	-3.155	-4.105
CHA/NiAl-LDH	24.60	76.27	+0.762	-0.102	-0.758

Initial Concentration (C_0) = 20 mg/L, dosages = 0.03 g, volume = 20 mL, ΔG = Gibbs free energy, ΔH = Enthalpy, ΔS = Entropy, CHA = Coconut Husk Ash, LDH = Layered Double Hydroxide

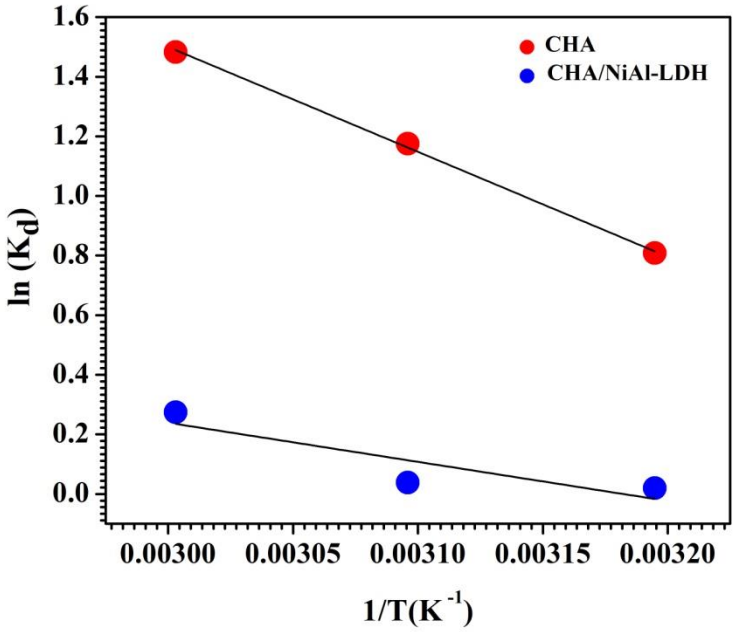

Fig V.7: Vant-Hoff plot for adsorption of methylene blue dye on to CHA and CHA/NiAl-LDH.

V.3.3 Effect of Dosages

The selection of suitable adsorption dosages is crucial. As a result, it is necessary to determine the optimum adsorbent dosages for the sorption process. The quantity of adsorbent added was varied from 0.010 g to 0.035 g. The experiment was performed at C_0 =40 mg/L, vol=20 mL, and time= 8 hrs. In **Fig V.8**, it is evident that with the increase in adsorbent dosages, the value of removal % increases from 83.43 to 99.21 % for CHA and 69.37 to 85.87 % for CHA/NiAl-LDH, respectively. The greater availability of free adsorption with increased dosages makes higher % removal possible. Moreover, the surplus of adsorbent applied beyond optimum values can lead to the accumulation of the sorbent particles, which retards the incoming adsorbate molecules towards the active site. From the graph, it shows 0.035 g as the most suitable dosage for the studied experimental conditions.[16,17]

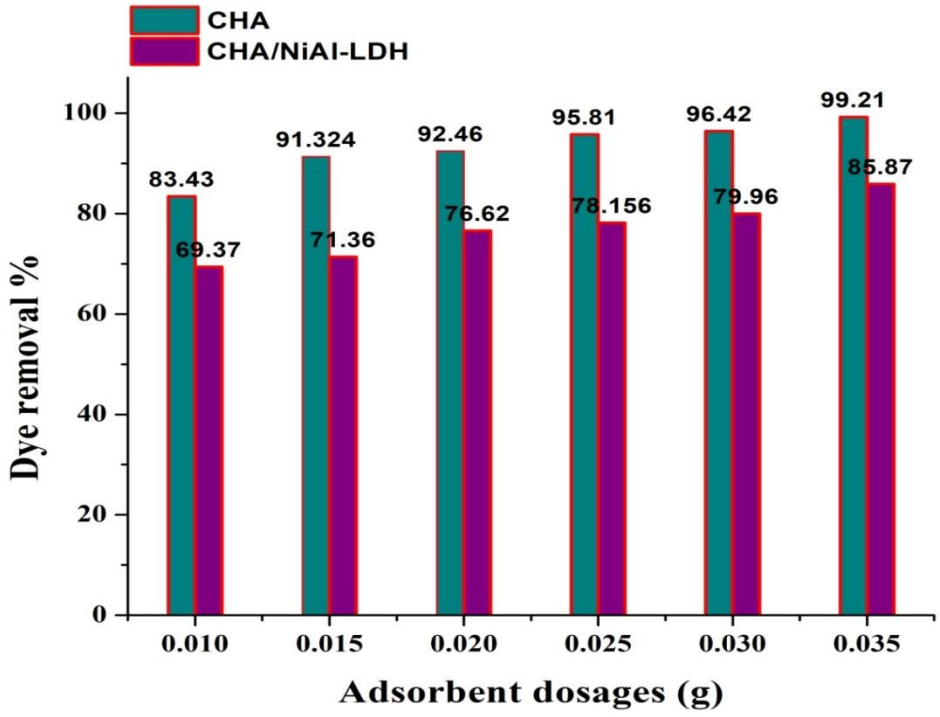

Fig V.8: Effect of adsorbent dosages on dye removal %.

V.3.4 Effect of Initial Dye Concentration

The influence of initial MB dye concentration on adsorption to CHA and CHA/NiAl-LDH was examined over a solute concentration ranging between (10-55 mg/L), which is presented in **Fig V.9(a, b)**. It is obvious that the equilibrium adsorption capacity (q_e) values increase with increased dye concentration for both adsorbents, CHA (q_e=12.09-23.03 mg/g) and CHA/NiAl-LDH (5.4-12 mg/g). At higher initial concentrations, the contact of the solute molecules with the adsorbent surfaces occurs significantly, which makes it more suitable for the adsorption process. Consequently, greater q_e values for adsorbing dye can be expected from the initial dye concentration.[18,19]

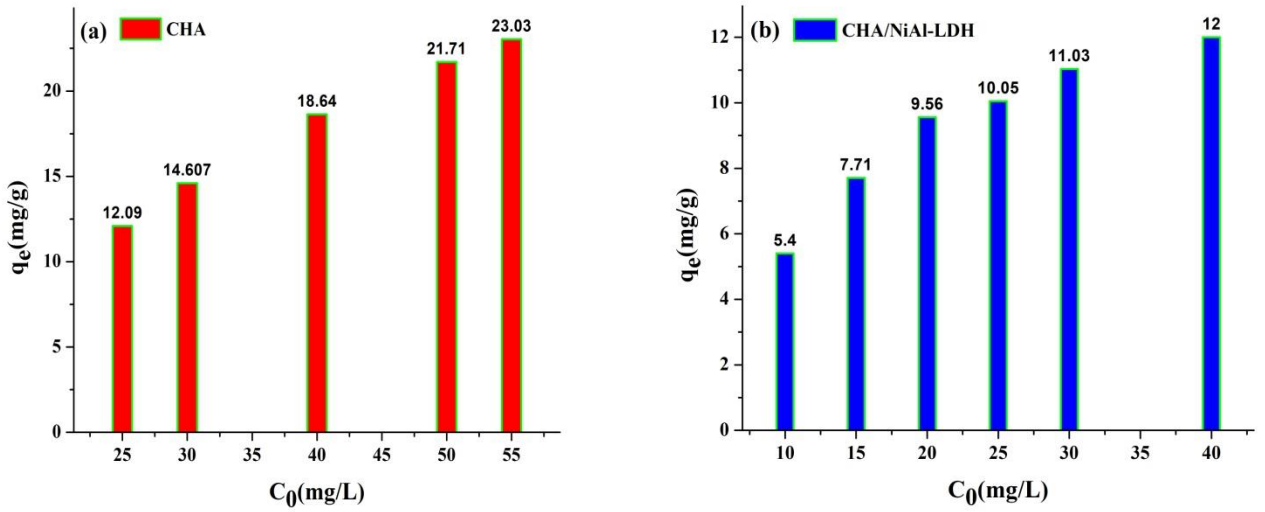

Fig V.9: Effect of initial concentration on the equilibrium adsorption capacity of (a) CHA (b) CHA/NiAl-LDH.

V.3.5 Effect of Contact Time

The contact time and the quantity of dye adsorbed (q_t) were analyzed under the experimental conditions of C_0= 10 mg/L, vol=40 mL, dosages= 0.035 g, and time= 20 mins. **Fig V.10** displays the function of q_t versus adsorption time. Generally, in most of the reported adsorbents, the graph shows the initial increases in q_t values with contact time, which are followed by gradual declination and attaining equilibrium stage.[20] In **Fig V.10**, the complete saturation of the curve for both adsorbents CHA and CHA/NiAl-LDH was achieved after 200 minutes. The bending of the curve observed after 40 mins of contact time was due to the transfer of surface-adsorbed MB dye onto the internal pores of the adsorbent, which causes a slow rate of adsorption. The maximum q_t values achieved at the contact time of 200 minutes for CHA and CHA/NiAl-LDH are 15.04, 12.76 mg/g, respectively.[21]

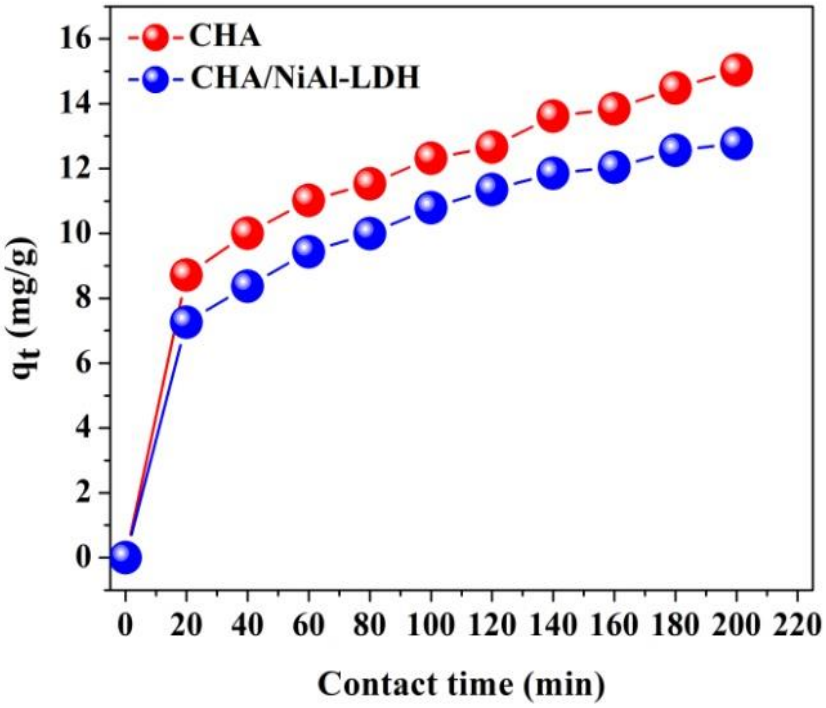

Fig V.10: Variation of q_t values with contact time.

V.3.6 Adsorption Isotherm Analysis

Fig V.11 (a, b) depicts the non-linear plot of isotherm data based on three models, and the isotherm parameters obtained are shown in **Table V.2**. From the analysis of all the isotherm data, the coefficient of determination (R^2) value was found to be greater in the Langmuir model (R^2=0.980) for CHA adsorbent, while for the CHA/NiAl-LDH Temkin model can be best accounted with R^2 value of 0.964. The maximum adsorption capacity q_{max} (mg/g) for the sorption of methylene blue by CHA and CHA/NiAl-LDH was 32.12 and 11.82 mg/g, respectively. The higher values of the q_{max} value of CHA can be attributed to the presence of more negatively charge functional groups and the micro-mesopore characteristics of the adsorbent.[22,23] The plot of C_0 vs R_L is depicted in **Fig V.12(a, b)**. The determined value of R_L lies in the range of 0-1, thus indicating the favorability of the sorption process.

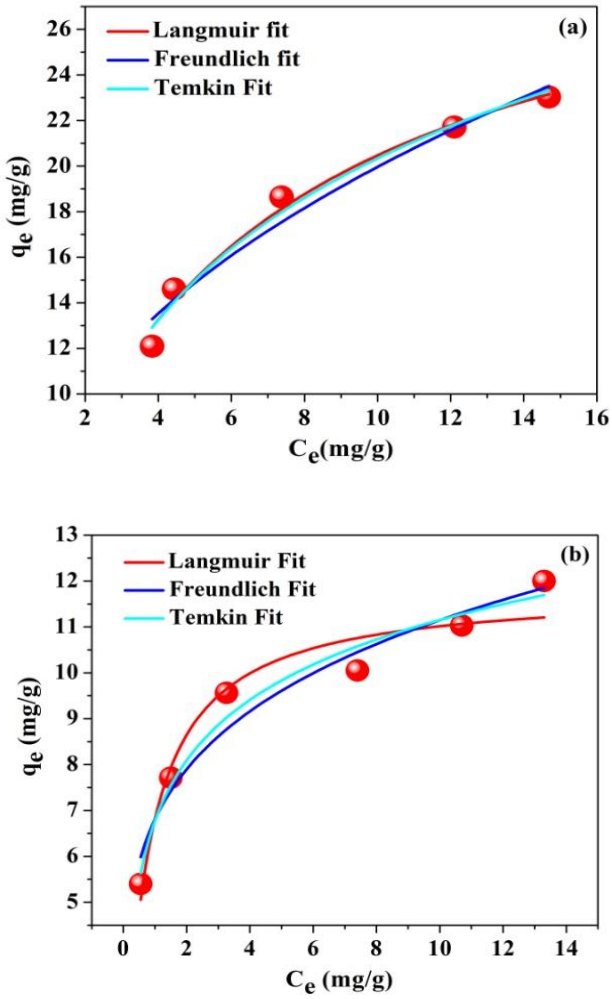

Fig V.11: Non-linear isotherm plot based on the Langmuir, Freundlich, and Temkin model for the adsorption of methylene blue over (a) CHA and (b) CHA/NiAl-LDH adsorbent.

Table V.2: Adsorption Isotherm parameters for the methylene blue adsorption.

		Adsorbents	
Isotherm model	**Constants**	**CHA**	**CHA/NiAl-LDH**
Langmuir	K_l (L/mg)	0.17559 ± 0.024	1.360 ± 0.258
	q_{max} (mg/g)	32.13 ± 1.76	11.82 ± 0.429
	R^2	0.980	0.942
Freundlich	n	2.354 ± 0.278	4.66 ± 0.576
	K_f (mg/g)(L/mg)$^{1/n}$	7.509 ± 0.856	6.80 ± 0.361
	R^2	0.952	0.942
Temkin	B_T	7.74 ± 0.597	1.90 ± 0.161
	K_T	1.38 ± 0.254	35.34 ± 15.16
	R^2	0.976	0.964

Initial Concentration (C_0) = 10-55 mg/L, dosages = 0.035 g, time = 4 h, q_{max} = adsorption capacity

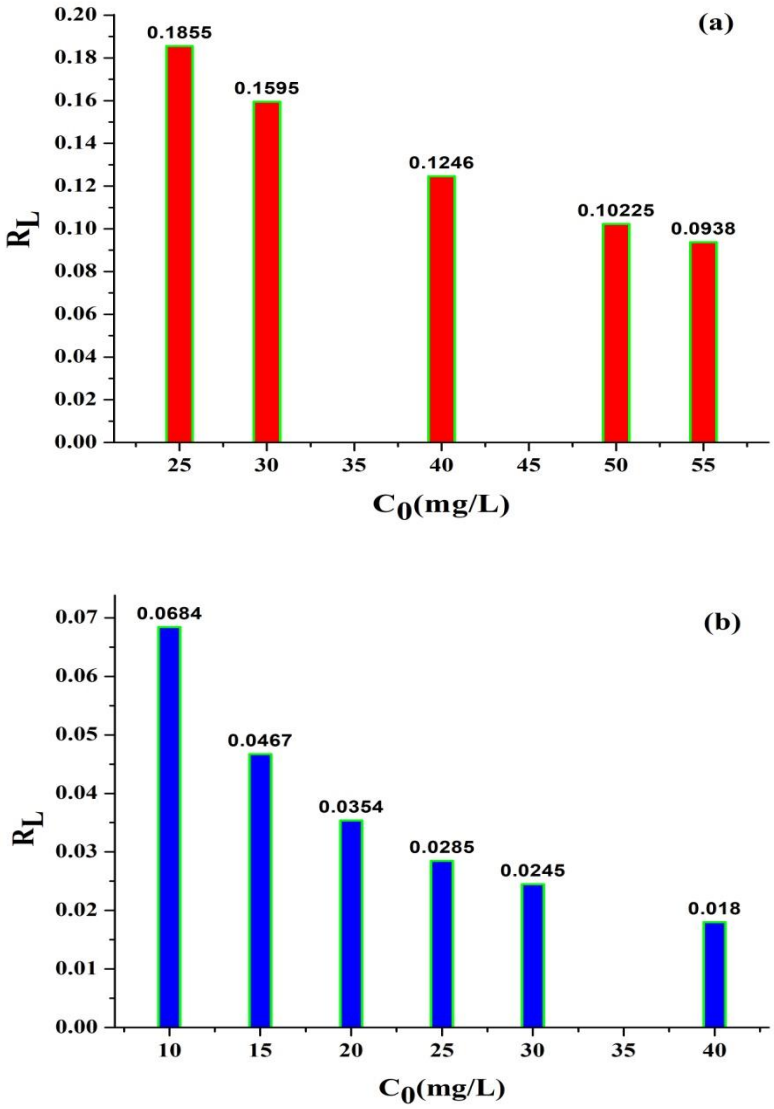

Fig.V.12: Plot of R_L vs C_0 for adsorbent (a) CHA and (b) CHA/NiAl-LDH.

V.3.7 Kinetic Data Analysis

The fits of the kinetics data based on the pseudo-first-order, pseudo-second-order, and intraparticle diffusion model is presented in **Fig V.13(a-c)**, and the evaluated parameters are summarized in **Table V.3**. The co-efficient of determination (R^2) value was used for predicting the best fit of the model. In **Table V.3**, it is manifested that the R^2 value obtained from the pseudo-second order is relatively closer to 1 than that from pseudo-first-order in both adsorbents. Therefore, it demonstrates that the pseudo-second-order model can best describe the kinetic

studies. In addition, the calculated values of q_{e2} are also closer to experimental q_e(mg/g) than q_{e1}.[24,25]

The graphical representation of the $q_t$vs $t^{0.5}$ plot shows a linear straight line. Since the straight line did not pass through the origin, the intraparticle diffusion model is not the rate-determining step during the sorption process of methylene blue by CHA and CHA/NiAl-LDH.[26]

Table.V.3: Adsorption kinetics parameters for methylene blue adsorption.

Kinetic model	Parameters	CHA	CHA/NiAl-LDH
	q_e (exp) mg.g^{-1}	15.36	13.29
Pseudo-first-order	q_{e1} (cal)	11.10	8.74
	K_1 (10^{-3}) min^{-1}	14.41	13.12
	Δq	0.092	0.114
	R^2	0.886	0.980
Pseudo-second-order	q_{e2} (cal)	16.52	14.32
	K_2 (10^{-4}) g.mg^{-1}.min^{-1}	21.37	24.36
	Δq	0.0251	0.0258
	R^2	0.988	0.993
Intraparticle diffusion	K_i	0.637	0.579
	C	5.917	4.816
	R^2	0.995	0.991

Experimental conditions: (Initial concentration (C_0) = (10 mg/L, dosages = 0.3 g, volume = 40 mL, time = 200 min) q_e (exp) = Experimental equilibrium adsorption capacity, q_{e1} (cal), q_{e2} (cal) = Calculated equilibrium adsorption capacity based on Pseudo-first-order and Pseudo-second-order kinetics model, respectively., K_1, K_2= Pseudo-first-order and pseudo-second-order rate constant, K_i = Intraparticle diffusion constant, C = Boundary layer thickness, Δq = Normalized standard deviation

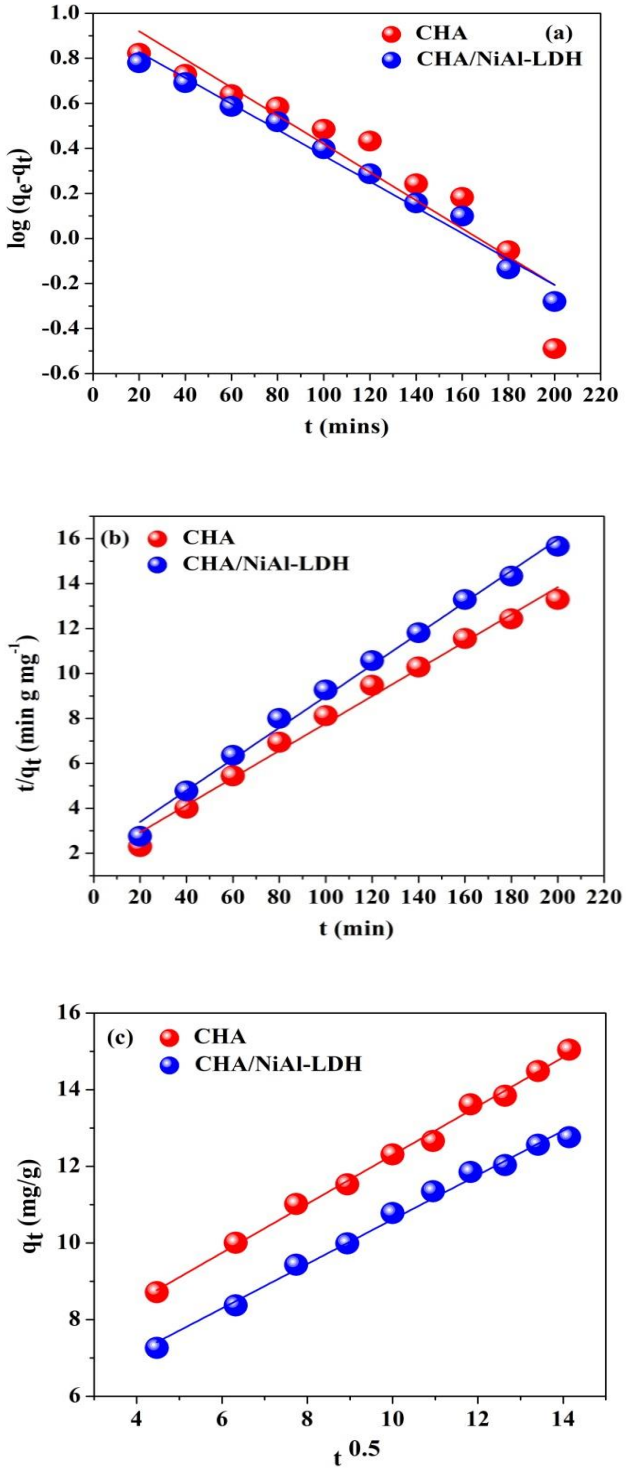

Fig.V.13: Linear adsorption kinetics plot (a) Pseudo-first order (b) Pseudo-second order and (c) Intraparticle diffusion

V.3.8 Adsorption Mechanism

The plausible mechanism for the adsorption of MB onto CHA and CHA/NiAl-LDH is not clear and involves intricate mechanism. However, the various interactions that can be speculated are H-bonding, electrostatic interaction, n-π, π-π, and pore filling. The aromaticity of the carbonaceous ash material is advantageous over the formation of π-π stacking and H-bonding with the organic pollutants. The π-π interaction occurs between the π ring of the adsorbent (CHA, CHA/NiAl-LDH) surface and the π aromatic ring of MB dye. The n-π interaction exists due to the presence of O-containing functional group (-OH, C-O) that can act as an electron donor to the π ring of MB.[8,27] Besides, H-bonding is possible between the positively charged N-atom of dye and the electronegative O atom of the adsorbent. In addition, inorganic components such as K, Ca, etc., can increase the hydrophilicity of dye. As evident from the FE-SEM images depicted in **Fig V.4**, the presence of pores on the adsorbent surface, which predicts the diffusion of dye molecules on the porous structure, could be possible.[28]

V.4 Conclusions

This study demonstrates the successful modification of NiAl-LDH with coconut husk ash and its adsorptive removal of methylene blue from the aqueous solution. Although, due to its positively charged LDH sheets, which caused repulsion, the pristine LDH does not remove cationic MB, fabrication with agricultural waste ash imparts ability to adsorb the targeted pollutant. The equilibrium isotherm and kinetic study envisage Langmuir and pseudo-second-order mechanisms. This study has provided a new pathway to synthesize LDH-ash composite materials to widen their adsorption properties over organic and inorganic pollutants of both cationic and anionic nature.

V.5 References

1. H. Halepoto, T. Gong, H. Memon, *Front. Environ. Sci.*, 10, **2022**, 1042256.
2. R. Al-Tohamy, S.S. Ali, F. Li, K.M. Okasha, Y.A.G. Mahmoud, T. Elsamahy, H. Jiao, Y. Fu, J. Sun, *Ecotoxicol Environ. Saf*., 231, **2022**, 113160.
3. P.O. Oladoye, T.O. Ajiboye, E.O. Omotola, O.J. Oyewola, *Results Eng*., 16, **2022**, 100678.
4. I. Khan, K. Saeed, I. Zekker, B. Zhang, A.H. Hendi, A. Ahmad, S. Ahmad, N. Zada, H. Ahmad, L.A. Shah, T. Shah, I. Khan, *Water*., 14, **2022**, 242.
5. J. Clifton II, J.B. Leikin, *Am. J. Ther*., 10, **2003**, 289.
6. F. Mashkoor, A. Nasar, *Cellulose*., 27, **2020**, 2613.
7. M. Khodale, N. Ghasemi, B. Moradi, M. Rahimi, *J. Chem*., **2013**, 383985.
8. D. Brahma, H. Nath, D. Borah, M. Debnath, H. Saikia, *Inorg Chem Commun*., 144, **2022**, 109878.
9. Z.M. Lazim, T. Hadibarata, M. Puteh, Z. Yusop, *Water Air Soil Pollut*., 226, **2015**, 34.
10. B.R. Freitas, J.O. Bragg, M.P. Orlandi, B.P. da Silva, I.V. Aoki, V.F.C. Lins, F. Cotting, *J. Mater. Res. Technol*., 19, **2022**, 1332.
11. S. Suman, S. Gautam, *Energy Sources, Part A: Recovery, Utilization, and Environmental Effects.*, 39, **2017**, 761.
12. M.F. Anuar, Y.W. Fen, M.H.M. Zaid, K.A. Matori, R.E.M. Khaidir, *Results Phys*., 11, **2018**, 1.
13. B.S. Yadav, S. Dasgupta, *Inorg Chem Commun*., 137, **2022**, 109203.
14. P.S. Kumar, P.S.A. Fernando, R.T. Ahmed, R. Srinath, M. Priyadharshini, A.M. Vignesh, A. Thanjiappan, *Chem Eng Commun*., 201, **2014**, 1526.
15. A.F. Hassan, G.A. El-Naggar, G. Esmail, W.A. Shaltout, *Appl. Surf. Sci. Adv*., 13, **2023**, 100388.
16. U.J. Etim, S.A. Umoren, U.M. Eduok, *J. Saudi Chem. Soc*., 20, **2016**, s-67.
17. M.Y. Chong, Y.J. Tam, *SN Appl. Sci*., 2, **2020**, 187.
18. P. Sharma, R. Kaur, C. Baskar, W.J. Chung, *Desalination*., 259, **2010**, 249.
19. M.H. Isa, L.S. Lang, F.A.H. Asaari, H.A. Aziz, N.A. Ramli, J.P.A. Dhas, *Dyes Pigm*., 74, **2007**, 446.

20. S. Dogar, S. Nayab, M.Q. Farooq, A. Said, R. Kamran, H. Duran, B. Yameen, *ACS Omega*., 5, **2020**, 15850.
21. N.T. Dinh, L.N.H. Vo, N.T.T. Tran, T.D. Phan, D.B. Nguyen, *RSC Adv*., 11, **2021**, 20292.
22. S. Sultana, K. Islam, M.A. Hasan, H.M.J. Khan, M.A.R. Khan, A. Deb, M.A. Raihan, M.W. Rahman, *Environ. Nanotechnol*., 17, **2022**, 100651.
23. O.S. Bello, K.A. Adegoke, S.O. Fagbenro, O.S. Lameed, *Appl. Water Sci*., 9, **2019**, 189.
24. V.P. Singh, A. Susaniya, S.C. Jain, R. Vaish, *J. Chem. Educ*., 98, **2021**, 3288.
25. T. Hongo, M. Moriura, Y. Hatada, H. Abiko, *ACS Omega*., 6, **2021**, 21604.
26. O.M. Paska, C. Pacurariu, S.G. Muntean, *RSC Adv*., 4, **2014**, 62621.
27. G.B. Balji, A. Surya, P. Govindaraj, G.M. Ponsakthi, *Inorg Chem Commun*., 143, **2022**, 109708.
28. H.N. Tran, Y.F. Wang, S.J. You, H.P. Chao, *Process Saf. Environ*., 107, **2017**, 168.